Journal of Experimental Botany, Vol. 70, No. 18 pp. 4887–4901, 2019
doi:10.1093/jxb/erz222 Advance Access Publication May 14, 2019
This paper is available online free of all access charges (see https://academic.oup.com/jxb/pages/openaccess for further details)

RESEARCH PAPER

Additive and epistatic interactions between *AKR* and *AIN* loci conferring bluegreen aphid resistance and hypersensitivity in *Medicago truncatula*

Lars G. Kamphuis[1,2,3], John P. Klingler[1,*] Silke Jacques[1,3], Ling-ling Gao[1], Owain R. Edwards[4] and Karam B. Singh[1,2,3,†]

[1] CSIRO Agriculture and Food, 147 Underwood Avenue, Floreat WA 6014, Australia
[2] UWA Institute of Agriculture, 35 Stirling Highway, Crawley WA 6009, Australia
[3] Curtin University, Centre for Crop and Disease Management, Kent Street, Bentley WA 6102, Australia
[4] CSIRO Land and Water, 147 Underwood Avenue, Floreat WA 6014, Australia

* Present address: NIMA, LLC, North Manchester, IN 46962, USA.
† Correspondence: karam.singh@csiro.au

Received 10 December 2018; Editorial decision 30 April 2019; Accepted 2 May 2019

Editor: : Robert Hancock, The James Hutton Institute

Abstract

Aphids, including the bluegreen aphid (BGA; *Acyrthosiphon kondoi*), are important pests in agriculture. Two BGA resistance genes have been identified in the model legume *Medicago truncatula*, namely *AKR* (*Acyrthosiphon kondoi* resistance) and *AIN* (*Acyrthosiphon* induced necrosis). In this study, progeny derived from a cross between a resistant accession named Jester and a highly susceptible accession named A20 were used to study the interaction between the *AKR* and *AIN* loci with respect to BGA performance and plant response to BGA infestation. These studies demonstrated that *AKR* and *AIN* have additive effects on the BGA resistance phenotype. However, *AKR* exerts dominant suppression epistasis on *AIN*-controlled macroscopic necrotic lesions. Nevertheless, both *AKR* and *AIN* condition production of H_2O_2 at the BGA feeding site. Electrical penetration graph analysis demonstrated that *AKR* prevents phloem sap ingestion, irrespective of the presence of *AIN*. Similarly, the jasmonic acid defense signaling pathway is recruited by *AKR*, irrespective of *AIN*. This research identifies an enhancement of aphid resistance through gene stacking, and insights into the interaction of distinct resistance genes against insect pests.

Keywords: Barrel medic, disease resistance, electrical penetration graph, jasmonic acid pathway, resistance gene interaction, salicylic acid pathway, sap-sucking insect.

Introduction

Aphids are major insect pests worldwide in both agricultural and horticultural production systems. They are notoriously difficult to control using insecticides as they are able to rapidly develop resistance to a range of different mode of action groups. These sap-sucking insects cause damage to agricultural and horticultural crops by ingesting nutrients from their host phloem sap; in addition, aphids vector many plant viruses. Genetic control of aphids through plant resistance (*R*) genes is a common pest management tool in many crops. Breeding programs cross such monogenic aphid resistance genes into plant germplasm and ensure resistance is retained in new plant varieties through marker-assisted selection. Despite their utility,

Abbreviations: AKR, *Acyrthosiphon kondoi* resistance; AIN, *Acyrthosiphon* induced necrosis; BGA, bluegreen aphid; EPG, electrical penetration graph; HR, hypersensitive response; JA, jasmonic acid; SA, salicylic acid

only two aphid resistance genes have been isolated and characterized: *Mi-1* from tomato, conferring resistance to the potato aphid (*Macrosiphum euphorbiae*; Rossi *et al.*, 1998), and *Vat* from melon, against the cotton-melon aphid (*Aphis gossypii*; Dogimont *et al.*, 2014; Boissot *et al.*, 2016). Both genes belong to the coiled-coil nucleotide-binding site-leucine-rich repeat (CC-NBS-LLR) class of resistance genes. Other aphid resistance genes have been identified, but not yet isolated, such as the *Rag* resistance genes in soybean (*Glycine max*) against the soybean aphid (*Aphis glycines*) (Hill *et al.*, 2017; O'Neal *et al.*, 2018) and the *Dn* resistance genes in wheat (*Triticum aestivum*) against the Russian wheat aphid (*Diuraphis noxia*) (Botha *et al.*, 2014). The *Ra* gene in lettuce, which confers resistance to the lettuce root aphid (*Pemphigus bursarius*), has also been shown through reverse genetics to be a member of the NLR family, contained within a large *R* gene cluster (Wroblewski *et al.*, 2007). In the model legume *Medicago truncatula* (barrel medic), a number of dominant aphid resistance genes have been identified, and these also reside in regions dense in NLR genes (reviewed by Kamphuis *et al.*, 2013*b*).

M. truncatula Gaertn is a model legume for basic research and a commercial pasture species subject to breeding in temperate regions of Australia. Several quantitative trait loci (QTLs) controlling antibiosis and tolerance to different aphid species have been identified (Guo *et al.*, 2012; Kamphuis *et al.*, 2012, 2013*a*) in addition to four major genes that confer aphid resistance (Klingler *et al.*, 2005, 2007, 2009; Gao *et al.*, 2008; Guo *et al.*, 2009, 2012; Stewart *et al.*, 2009; Kamphuis *et al.*, 2015). Two of these resistance genes, *AKR* (*Acyrthosiphon kondoi* resistance) and *AIN* (*Acyrthosiphon* induced necrosis) confer resistance against the bluegreen aphid (*Acyrthosiphon kondoi* Shinji; BGA). *AKR* was identified as a dominant gene in resistant cv. Jester (Klingler *et al.*, 2005), whereas the *AIN* gene was identified in the reference genotype Jemalong-A17 (hereafter referred to as A17) (Klingler *et al.*, 2009), which is near isogenic with Jester, sharing 89% genome sequence identity. *AKR* is a dominant resistance gene which conditions both antibiosis and antixenosis, with resistance operating at the phloem level (Klingler *et al.*, 2005). *AIN* is dominant with respect to presence versus absence of necrotic lesions in response to BGA and pea aphid (*Acyrthosiphon pisum*), yet exhibits incomplete dominance with respect to the degree of damage and level of resistance to BGA (Klingler *et al* 2009). *AIN* is also responsible for the reduction of aphid biomass for both BGA and pea aphid, albeit to a lesser degree for pea aphid compared with BGA (Guo *et al.*, 2012), and also conditions a hypersensitive response (HR) to both aphid species (Klingler *et al.*, 2009; Guo *et al.*, 2012). While *M. truncatula* accession Jester contains both the *AKR* and *AIN* genes, the reference accession A17 only contains the *AIN* gene (Klingler *et al.*, 2009). An additional reference genotype of *M. truncatula*, A20, is highly susceptible to BGA and contains neither of these resistance genes (Klingler *et al.*, 2005, 2009; Guo *et al.*, 2012). The presence of two aphid resistance genes against BGA in Jester raises questions about their relative contributions to this cultivar's high level of BGA resistance.

The details of molecular events during plant–aphid interactions show parallels with models for plant–microbe interactions (reviewed by Goggin, 2007; Walling, 2008; Kamphuis *et al.*, 2013*b*; Zust and Agrawal, 2016). Progress has been made in understanding the defense signaling pathways that operate during *R* gene-mediated resistance to aphids using comparative transcriptome analyses (Martinez de Ilarduya *et al.*, 2003; Thompson and Goggin, 2006; Gao *et al.*, 2007*a*; Li *et al.*, 2008; Jaouannet *et al.*, 2015; Escudero-Martinez *et al.*, 2017; Song *et al.*, 2017) and transcription factor profiling (Gao *et al.*, 2010). Although particular transcript profiles vary substantially among different plant–aphid species combinations, gene expression studies have shown that aphids elicit plant defense networks controlled by hormones such as salicylic acid (SA), jasmonic acid (JA), and ethylene (ET) (Zust and Agrawal, 2016). Transcriptional changes in the SA, JA, and ET defense pathways have been observed following BGA infestation in *M. truncatula* (Gao *et al.*, 2007*a*), where genes in the octadecanoid pathway leading to the synthesis of JA were exclusively and highly induced in cultivar Jester or in A17^{+AKR}, which is an A17 line with a small introgression harboring the *AKR* gene. In contrast, genes in the SA and ET pathways were induced in a similar fashion in A17 and Jester.

This study investigates interactions between the *AKR* and *AIN* loci with respect to BGA performance and plant response to BGA infestation. Furthermore, it examines the roles of the JA and SA defense signaling pathways identified by Gao *et al.* (2007*a*) following BGA infestation in the presence of the different haplotypes of the resistance genes *AKR* and *AIN*. Using recombinant haplotypes, we demonstrate that *AKR* and *AIN* have additive effects on resistance to BGA colonization and that *AKR* is able to suppress *AIN*-controlled macroscopic necrotic lesions. Through electrical penetration graph (EPG) analysis, we show that lines harboring *AKR* have reduced phloem sap ingestion, consistent with a model of phloem-based, JA pathway-dependent resistance. The genetic interactions identified between the two resistance loci indicate a complex interplay between JA signaling and HR to potentiate aphid resistance.

Materials and methods

Plants and aphids

Plants used in this study were *M. truncatula* genotypes Jester, A17, and A20, and progeny derived from crosses between Jester and A20, generated using a manual crossing procedure as described previously (Kamphuis *et al.*, 2007). A list of the Jester×A20-derived F_3 families with different allelic combinations of the *AKR* and *AIN* resistance genes can be found in Supplementary Table S1 at *JXB* online. Prior to laboratory or greenhouse experiments, seeds were scarified and germinated in the dark on moist filter paper, then kept at 4 °C for 10–14 d to synchronize radicle growth before transfer to soil. For the gene expression and aphid feeding behavior experiments, plants were grown in 1.2 liter pots in a growth chamber (14 h light at 22 °C and 10 h dark at 20 °C under high-pressure sodium and incandescent light at 225–250 μmol m^{-2} s^{-1}). The aphid phenotyping experiments were conducted with plants grown in 1.2 liter pots in natural light in a greenhouse with temperatures ranging from 15 °C to 30 °C. The aphids used in this study were an asexual, parthenogenetic strain of BGA collected from narrow-leafed lupin in Western Australia, derived from a single aphid, and cultured in the laboratory on the susceptible subclover (*Trifolium subterraneum*) variety Dalkeith as described by Gao *et al.* (2007*b*). Aphids were transferred to experimental plants with a fine paintbrush.

Test for BGA resistance in Jester×A20 F_2 and $F_{2:3}$ progeny

Individual progeny from the Jester×A20 F_2 population were phenotyped for BGA resistance as described by Klingler *et al* (2005). Two-week-old plants were infested with three apterous adults and, 3 weeks after infestation, the parents and each F_2 plant were given a subjective score on a scale from 1 to 5 for the amount of aphid-induced stunting and leaf damage. Low values indicated little or no visible damage, while high values indicated severe stunting and necrosis. Phenotyped F_2 plants were genotyped with molecular markers to identify suitable progenitors for $F_{2:3}$ progeny in a further round of testing for BGA resistance phenotype. In addition to the aphid colonization level, plants were examined for the presence or absence of necrotic lesions that are characteristic of BGA-infested A17 (Klingler *et al* 2009).

Molecular marker analysis

Genomic DNA samples from Jester, A20, their phenotyped F_2 progeny, and selected $F_{2:3}$ progeny were genotyped for molecular polymorphisms segregating on chromosome 3 and flanking the regions harboring *AKR* and *AIN*, using cleaved amplified polymorphic site (CAPS) and simple sequence repeat (SSR) markers developed by the *Medicago* genome sequencing project (http://www.medicagohapmap.org/?genome). PCRs, restriction enzyme digestion (if necessary), and gel electrophoresis for the polymorphic markers were conducted as described by Klingler *et al.* (2005). Results identified F_2 and homozygous $F_{2:3}$ progeny with recombination events between *AKR* and *AIN*, to determine which plants were suitable as progenitors for haplotypic analysis of BGA resistance in the $F_{3:4}$ generation. (Supplementary Table S1). A graphical depiction of recombinant haplotypes for the *AKR* and *AIN* loci on chromosome 3 is shown in Fig. 1.

Plant–aphid interaction in $F_{3:4}$ families

Eight individual seedlings were grown in separate pots for each $F_{3:4}$ family member, and for Jester, A17, and A20. Two weeks after sowing, each plant was infested with two adult apterae in a growth chamber at 22 °C with a 16 h photoperiod, and covered with a ventilated, whole-plant bottle cage according to the method of Klingler *et al.* (2009). Infested plants were immediately returned to their positions in the growth chamber in a completely randomized design. Nineteen days after infestation, the bottles were removed and damage symptoms were recorded. Aphids on each plant were gently brushed off and immediately weighed. Above-ground plant tissue was removed, dried, and weighed. Differences in haplotypic means were analyzed with Dunn's test.

3,3′-Diaminobenzidine (DAB) staining to visualize H_2O_2 production

Three plants from each $F_{3:4}$ family of every haplotype as well as the genotypes Jester, A17, and A20 were infested on the second fully expanded trifoliate leaf with 16 adult apterae, confined to leaf cages. An equal number of plants received aphid-free cages to serve as negative controls. Three days after infestation, when all infested leaves of A17 were beginning to show macroscopic lesions induced by BGA, the caged leaves were excised, aphids were removed, and leaves were DAB stained for H_2O_2 production as described previously (Klingler *et al.*, 2009). DAB staining was quantified relative to the total leaf area using the MIPAR software package to process the DAB-stained leaf images (Sosa *et al.*, 2014).

Aphid feeding behavior

The feeding behavior of BGA on the plants with different allelic combinations of *AKR* and *AIN* was conducted using the direct-current electrical penetration graph (EPG) technique (Tjallingii, 1978) as described in Klingler *et al.* (2005). Four-week-old plants were infested with a single apterous BGA adult placed on a single trifoliate leaf and the feeding behavior was monitored over an 8 h period. A minimum of 12 biological replicates were included for each haplotype, with at least three distinct lines originating from the Jester×A20 cross per haplotype. An eight channel amplifier (Giga-8d) simultaneously recorded eight individual aphids on separate plants, two for each combination of *AKR–AIN*, *AKR–ain*, *akr–AIN*, and *akr–ain* over an 8 h period. Data acquisition and analysis of EPG signals was performed via the Stylet + windows-based software package (EPG systems, Wageningen, The Netherlands).

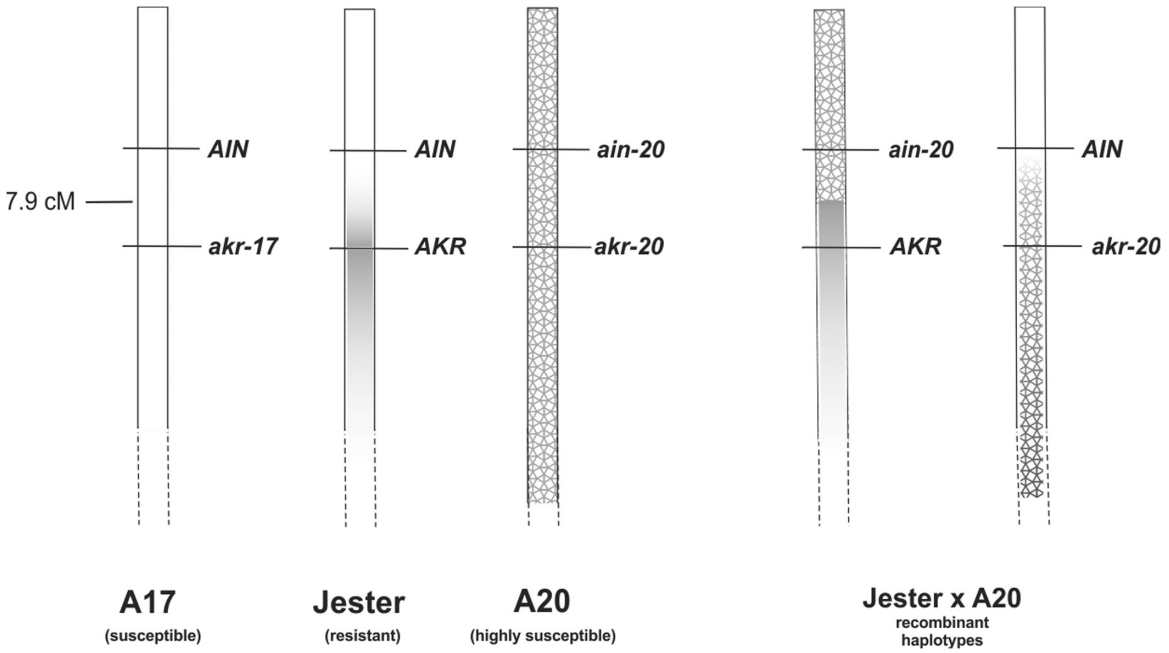

Fig. 1. Chromosome 3 haplotypes of *M. truncatula* lines tested for BGA resistance. The positions of the *AKR* and *AIN* loci are indicated on each chromosome. The shading in the Jester chromosome indicates the region of introgression into the A17 genetic background, based on DNA polymorphism analysis. The hatched pattern in the A20 chromosome indicates a haplotype genetically distinct from the reference genotype A17 (chromosome shown in white) and from Jester. Jester×A20 F_2 plants with recombination events between the *AKR* and *AIN* loci were used to generate experimental lines with different homozygous combinations of the two loci.

Waveform patterns in this study were uploaded into the EPG analysis + platform and manually assigned to waveform labels corresponding to the categories described by Tjallingii and Hogen Esch (1993). The main waveform categories are: np, non pathway; c, pathway; E1, salivation into phloem; E2, phloem sap ingestion; F, derailed stylet; G, xylem drinking. The mean proportion of time spent in each behavior on each plant of the four haplotypes was analyzed by two-sample *t*-tests ($P<0.05$) and an overview of the *t*-test results are summarized in Supplementary Table S2.

RNA isolation, DNA synthesis, and quantitative reverse transcription–PCR (RT–qPCR) conditions

RNA isolation and cDNA synthesis were performed using the Purescript RNA isolation kit (Gentra Systems, Minneapolis, MN, USA) and the Invitrogen Superscript III reverse transcriptase kit (Invitrogen) as described by Gao *et al.* (2007*a*). RT–qPCR was performed using an iCycler (Bio-Rad Inc., Hercules, CA, USA), with the thermal profile 95 °C for 2.5 min; 40 cycles of 95 °C for 15 s, 60° C for 30 s, and 72 °C for 30 s; followed by a melt curve program of 70 °C to 95 °C, with 0.5 °C increase per cycle. In order to compare data from different PCR runs or cDNA samples, threshold cycle (C_T) values for all selected genes were normalized to the C_T value of a tubulin gene (as described by Gao *et al.*, 2007*a*), whose expression remained constant among various aphid-infested and non-infested tissues (results not shown). Relative gene expression was derived from using $2^{-\Delta CT}$, where ΔC_T represents the C_T of the gene of interest minus the C_T of tubulin. The significance in difference between ratios was analyzed using a Tukey honestly significant difference (HSD) test, using JMP 7.0 software (SAS Institute Inc).

Results

AKR *exerts dominant suppression epistasis on* AIN-*controlled macroscopic necrotic lesions*

Previous work on mapping *AKR* employed two F_2 populations, one from the cross A17×Jester, and another from the cross Jester×A20 (Klingler *et al.*, 2005). To increase mapping resolution of *AKR* in the Jester×20 population, a set of $F_{2:3}$ families was tested for BGA resistance; these families were selected because genomes of their F_2 progenitors had recombination events near the *AKR* locus (Table 1). Upon infestation with BGA, two such families showed reactions unlike that of either parent, Jester or A20; the response was instead similar to the BGA-induced macroscopic HR and stunting observed in A17, conferred by the *AIN* locus (Klingler *et al.*, 2005, 2009; Table 1). These two families segregated for Jester-like resistance and A17-like susceptibility in a 3:1 ratio, without the recovery of any A20-like plants among the progeny. This rare appearance of A17-like plants suggested action by *AIN*, consistent with the observation that Jester and the near-isogenic A17 share identical molecular marker haplotypes surrounding the *AIN* locus. The *AKR* and *AIN* loci are separated by a mere 7.9 cM on chromosome 3, an interval that, in cv. Jester, happens to include the boundary of the introgressed chromosome segment harboring *AKR*. This segment was introduced from a wild donor accession into Jester by recurrent backcrossing to A17 (Hill, 2000; Klingler *et al.*, 2005; Gao *et al.*, 2007*a*; unpublished data). This small genetic distance makes recombination events between these loci relatively rare in the Jester×A20 F_2 population.

Collectively, these results suggest an epistatic interaction between the two aphid resistance genes, *AKR* and *AIN*, in resistant cv. Jester. To investigate this interaction, an additional round of BGA resistance phenotyping was performed in the Jester×A20 population, using a sample size of 142 F_2 plants. In this experiment, all infested F_2 plants were scored for resistance, and also carefully examined for the presence of any BGA-induced necrotic lesions resembling those appearing

Table 1. *Molecular marker genotypes and BGA resistance phenotypes of Jester×A20 F_2 progenitor plants, and phenotypes of $F_{2:3}$ progeny after infestation with BGA*

F_2 plant	BGAphenotype	*AKR*		*AIN*				F_3 phenotypes		
		h2_6g9b	38K1L	003A03	34TC15	003G03	004A05	A20	A17	Jester
063	S	A	A	A	A	A	H	18	0	0
031	S	A	A	A	H	H	H	13	5	0
057	S	A	A	A	H	H	H	13	5	0
004	S	A	A	H	H	H	H	14	4	0
116	S	A	A	H	H	H	H	13	5	0
029	R	H	H	A	A	A	A	0	0	18
034	R	H	H	A	A	A	A	0	0	18
048	R	H	H	H	H	A	A	0	0	18
052	R	H	H	H	A	A	A	6	0	12
123	R	H	H	H	A	A	A	3	0	15
125	R	H	H	H	B	B	B	0	3	15
020	R	H	H	H	H	H	A	7	0	11
024	R	H	H	H	H	H	B	2	0	16
039	R	H	H	H	H	H	A	0	0	18
099	R	H	H	H	H	H	A	5	0	13
137	R	H	H	H	H	H	B	7	0	11

Molecular markers are listed in order of their linkage relationships on chromosome 3. Marker codes are as follows: A, homozygous for A20 alleles; B, homozygous for Jester alleles; H, heterozygous. F_2 plants highlighted in bold were the only plants out of 142 to show A17-like damage symptoms in response to BGA, and were also the only plants homozygous for A20 alleles at the *AKR* locus and heterozygous at the *AIN* locus. Figures in columns labeled with inbred lines A20, A17, and Jester indicate the number of $F_{2:3}$ progeny showing BGA-related phenotypes similar to the corresponding line.

in genotype A17. This was in contrast to previous rounds of testing in which plants were qualitatively scored as resistant or susceptible, based on a pronounced difference in aphid colonization reflected in the parental lines.

Three weeks after infestation, plants were assessed for BGA resistance as described by Klingler *et al.* (2005). The resistant:susceptible ratio of F_2 plants was consistent with 3:1 segregation for the dominant *AKR* gene (113 resistant:29 susceptible; χ^2=1.59; *P*=0.21), with the 113 resistant individuals not showing any necrotic lesions. Interestingly, four of the 29 susceptible plants showed necrotic lesions and stunting symptoms quite similar to those observed in A17 plants that were used as controls in this experiment.

The observed phenotypic ratios suggest a model of dominant suppression epistasis of the *AKR* gene on *AIN*, with the assumption that both genes are dominant. *AKR* was shown to be dominant by Klingler *et al.* (2005); *AIN* was shown to be dominant with respect to the presence or absence of necrotic lesions, but semi-dominant with respect to the degree of this damage (Klingler *et al.*, 2009). This hypothesis of gene interaction was tested using two alternative models in which progeny arise from a dihybrid cross, as in the F_2 population from Jester×A20 (Table 2). In the first model, which proposes an independent assortment of unlinked loci (*AKR* and another unknown locus), a 13:3 ratio of non-necrotic:necrosis-expressing plants would be expected upon infestation of F_2 plants with BGA. In the second model, a distance of 7.9 cM between *AKR* and another locus (the known distance to *AIN*) is considered. In this model, a much lower frequency of only 3.8%, or 5.4 plants out of 142, would be expected to exhibit a BGA-induced necrosis. Since the latter model is consistent with the observed frequency of four plants in this category, as opposed to the 29 plants with model one involving an independent assortment of unlinked loci, we conclude that *AKR* exerts dominant suppression epistasis on *AIN*, with respect to the necrosis phenotype.

The effects of AKR *and* AIN *on BGA resistance are additive*

Since Jester was found to contain two BGA resistance genes, *AKR* from a donor accession and *AIN* from its recurrent parent and near-isogenic A17, this raised the question of whether *AIN* may influence *AKR*-mediated BGA resistance in Jester, particularly since *AKR* appears to block the *AIN*-mediated macroscopic HR and stunting seen in A17 during BGA colonization. A genetic dissection of the effects of the *AKR* and *AIN* genes on BGA resistance was undertaken by selecting Jester×A20 F_2 progeny with recombination events inside the 7.9 cM interval separating these loci. Seed from these F_2 plants were collected, and $F_{2:3}$ families from these individuals were tested for BGA resistance and again genotyped with diagnostic molecular markers to confirm their homozygosity at each locus, with 18 plants tested per $F_{2:3}$ family (Table 1). In all cases, individual F_3 plants showed phenotypes that matched their expected molecular marker genotypes for markers tightly linked to the *AKR* and *AIN* loci. In most cases, the ratios of different phenotypic categories were consistent with segregation of a dominant gene. In three cases (families from F_2 progenitors 029, 034, and 048), no A17-like plants were observed out of the 18 plants sampled, even though the molecular marker data indicated that they were segregating for the *AKR* gene. Nevertheless, all of these F_3 plants showed segregation at the *AKR* locus that corresponded to the observed resistant phenotypes; no plants homozygous for A20 alleles at the *AKR* locus were recovered. Individual $F_{2:3}$ progeny showing BGA resistance or susceptibility and homozygosity at each locus of interest were grown to maturity and their F_4 generation seed were collected for further experiments. Four separate $F_{3:4}$ families representing each of four distinct classes, or haplotypes, were chosen for BGA infestation. These haplotypic classes were defined as *akr–ain* (similar to parental line A20); *akr–AIN* (similar to reference genotype A17); *AKR–ain* (unlike any line that had been tested); and *AKR–AIN* (similar to parental line Jester).

Genotypes A20 and Jester are genetically unrelated and highly polymorphic; the sampling of four separate $F_{3:4}$ families of each haplotype was designed to average out variability from other parts of the genome, outside of the *AKR* and *AIN* loci, that might exert smaller effects on the BGA–plant interaction.

The results of this infestation experiment are summarized in Fig. 2. Since genotypes A20 and A17 have heritable differences in biomass, even in the absence of aphids (Klingler *et al.*, 2009), it is appropriate to standardize aphid resistance by expressing the phenotype in terms of aphid colony weight standardized for plant biomass. Colony weight, plant dry weight, and colony weight per plant weight were all clearly affected by plant haplotype, with the least resistant plants possessing neither resistance gene, while the most resistant plants possessed both genes. In general, the haplotype of each inbred line resembled the phenotypes of the $F_{3:4}$ families of the corresponding haplotype (Fig. 2A). The presence of both resistance genes correlated with the high level of BGA resistance in Jester. Members of the *akr–AIN* haplotype showed lower plant dry weights than the other haplotypes, and the grand mean for this haplotype was significantly lower than that of the *akr–ain* families. The *akr–AIN* haplotype was also the only one to exhibit macroscopic HR and stunting in response to BGA, with all plants in this category showing pronounced BGA-induced damage.

A comparison of the grand means of $F_{3:4}$ families for each haplotype shows an interesting pattern with respect to colony

Table 2. *Test of models for dominant suppression epistasis of* AKR *on* AIN *in a population of 142 F_2 plants from the cross Jester×A20.*

Genetic model	Expected ratio of infested plants non-necrotic: necrotic	Expected number of plants with necrosis out of 142	Observed number of plants with necrosis	χ^2 value	*P*-value
Independent assortment	13:3	26.6	4	23.66	<0.00001
Linkage of 7.9 cM	75.95:3	5.4		0.38	0.554

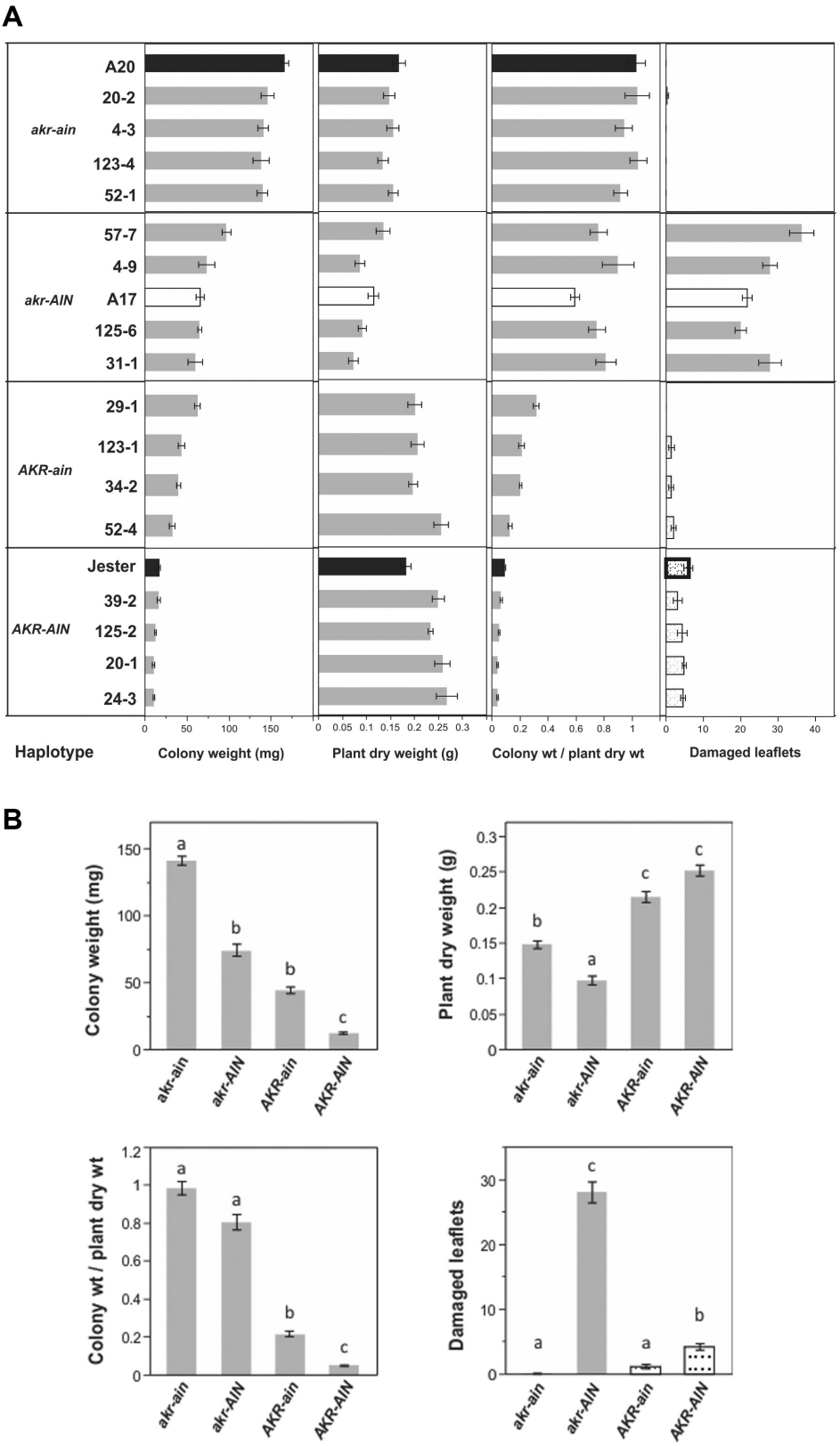

Fig. 2. Effects of plant haplotype on BGA colony development and infested plant weight. Four different $F_{3:4}$ families from the cross Jester×A20 are shown for each combination of *AKR* and *AIN* genes (A). In (A), bars indicate means (±SE) of eight replicate plants for each $F_{3:4}$ family or inbred line. Gray bars, $F_{3:4}$ families; black bars, parental genotypes; white bars, reference genotype A17. In (B), grand means are reported for only the $F_{3:4}$ families, categorized by haplotype. Bars represent means (±SE) of 32 replicate plants for each haplotype. Stippled bars represent *AKR*-containing plants that had only small, chlorotic flecks, rather than necrosis, in response to BGA. Different letters indicate significant differences, based on Dunn's test for all pairs with joint ranking (P<0.05).

weight per plant dry weight (Fig. 2B). The decline in this ratio by the addition of the *AIN* gene to the *akr* background is similar to the fractional decline by the addition of the *AIN* gene to the *AKR* background: 0.18 units separate the *akr–ain* and the *akr–AIN* haplotypes, while 0.17 units separate the *AKR–ain* and the *AKR–AIN* haplotypes. These strikingly similar numbers suggest that the effects of the two genes on BGA resistance are additive.

Interestingly, nearly all plants of the *AKR–AIN* haplotype, including resistant line Jester, had leaves with faint, chlorotic flecks similar to those of A17 during the earliest visible stage of BGA-induced HR (Fig. 2B). In contrast, nearly all *akr–AIN* plants had leaves with pronounced necrotic lesions or even death of complete leaflets or trifoliate leaves. Virtually none of the plants lacking the *AIN* gene had any type of chlorotic or necrotic lesions. These results are consistent with the findings of Klingler *et al.* (2009), wherein the *AIN* gene mediates a HR to BGA.

AKR *inhibits the formation of macroscopic necrotic lesions, but does promote localized production of* H_2O_2

Leaf images of individual, caged leaves from representative $F_{3:4}$ families following 3 d of infestation with BGA indicate the presence of small chlorotic flecks produced in leaves of the *AKR–AIN* (Fig. 3A, D) and *AKR–ain* (Fig. 3B, C, E, F) haplotypes and are circled in red. When only the *AIN* locus is present, macroscopic necrotic lesions can be observed after BGA infestation (Fig. 3H, I). Subsequent DAB staining was performed on a different set of individual leaves of plants infested with BGA using the method of Klingler *et al.* (2009) (Fig. 4). Reddish-brown staining by DAB indicates the localized production of H_2O_2, indicative of an oxidative burst associated with a HR (Thordal-Christensen *et al.*, 1997; Orozco-Cardenas and Ryan, 1999). DAB staining in haplotypes containing the *AKR* locus showed small, punctate flecks that suggest probe locations by BGA (Fig. 4A–C). Control plants that were not infested with BGA showed no such staining (data not shown). Relative quantification of the DAB staining with the MIPAR software package (Sosa *et al.*, 2014) showed clear differences in percentage DAB staining area versus total leaf area for the different haplotypes (Supplementary Fig. S1). The presence of *AKR* led to a reduction of DAB staining, with an average of 5.3% DAB stain (Supplementary Fig. S1A–C) compared with lines carrying *AIN* only where the necrotic lesions account for 11.9% of DAB stain (Supplementary Fig. S1E, F). It is intriguing that the *AKR* gene alone appeared to condition chlorotic fleck formation as well as resistance to BGA, although the H_2O_2 production did not lead to the formation of macroscopic necrosis as seen in plants possessing *AIN* (Figs 3H, I, 4E, F). Thus, BGA elicited small chlorotic lesions in the *AKR* background, yet the *AKR* gene inhibited the transition from small chlorotic flecks to larger, fully necrotic lesions in the presence of *AIN*, consistent with a model of dominant suppression epistasis.

To validate the production of H_2O_2 further, the expression of four genes associated with H_2O_2 metabolism was investigated in A20, A17, and Jester plants (Fig. 5). Following BGA infestation of A17 and Jester, *Respiratory burst oxidase homolog-1* (*RBOH-1*), *Respiratory burst oxidase homolog-2* (*RBOH-2*), and a *Peroxidase* (*PXY*) were significantly induced compared with their uninfested counterparts and A20-infested and uninfested plants (Fig. 5A–C). A *Superoxide dismutase* (*SDCZ*) was differentially expressed in Jester-infested petioles compared with all other treatments at 36 h post-infestation (Fig. 5D). There is thus recruitment of H_2O_2-associated genes in genetic backgrounds that carry *AKR* and *AIN*.

EPG analysis shows a significant reduction in phloem feeding on lines harboring AKR

The EPG technique allows real-time observation of phloem feeding behavior by insects. Previously we demonstrated that BGA has significantly less phloem sap ingestion on Jester plants (harboring both *AKR* and *AIN*) compared with A17 (harboring *AIN* only) (Klingler *et al.*, 2005). This thus raised the question of whether BGA has less phloem contact on lines containing both *AKR* and *AIN* compared with those only containing the *AKR* locus. Although BGA attempted to engage in feeding in the *AKR–AIN* haplotype by salivating into the phloem (1%), it did not reach the stage of actual phloem sap ingestion (Fig. 6). The absence of *AIN* in *AKR–ain* plants corresponded to an increase in time spent in phloem ingestion (3% versus 0% in *AKR–AIN* plants), although this difference was statistically non-significant. However, significant differences ($P<0.05$) were observed between the lines harboring *AKR* (*AKR–AIN* and *AKR–ain* haplotypes) and the lines lacking *AKR* (*akr–AIN* and *akr–ain* haplotypes) in non-pathway and phloem sap ingestion waveform patterns, with aphids spending up to 44% of their time not penetrating the leaves of *AKR*-containing lines. In contrast, up to 24% of the 8 h was spent on phloem feeding in lines lacking *AKR*. Our results suggest that only the presence of *AKR* is essential to inhibit phloem sap feeding, irrespective of the presence/absence of *AIN*.

Basal resistance in M. truncatula *A20 does not involve the recruitment of JA signaling, but does recruit certain SA-regulated genes*

Gao *et al.* (2007*a*) compared BGA-induced gene expression between A17 and Jester, and concluded that, while SA signaling is activated in both near-isogenic lines, JA signaling is exclusively activated in Jester, not A17, showing that *AKR*-mediated resistance to BGA in Jester involves JA signaling. To determine the role of these defense signaling pathways in basal resistance in the accession A20, the transcriptional changes of JA- and SA-responsive genes were investigated and compared with those of A17 and Jester. Sampling of leaf RNA at 36 h after BGA infestation showed no transcriptional change of the SA-regulated genes *PR10*, *PR5*, and *BGL* in A20, whereas significant increases in transcript abundance were observed for these three genes in A17 and Jester (Fig. 7). For all three genes, significantly higher transcript abundances were observed in Jester compared with A17 in accordance with our previous observations where the strongest expression of the JA- and SA-responsive genes was observed at 36 h post-aphid infestation (Gao *et al.*, 2007*a*). In contrast to these

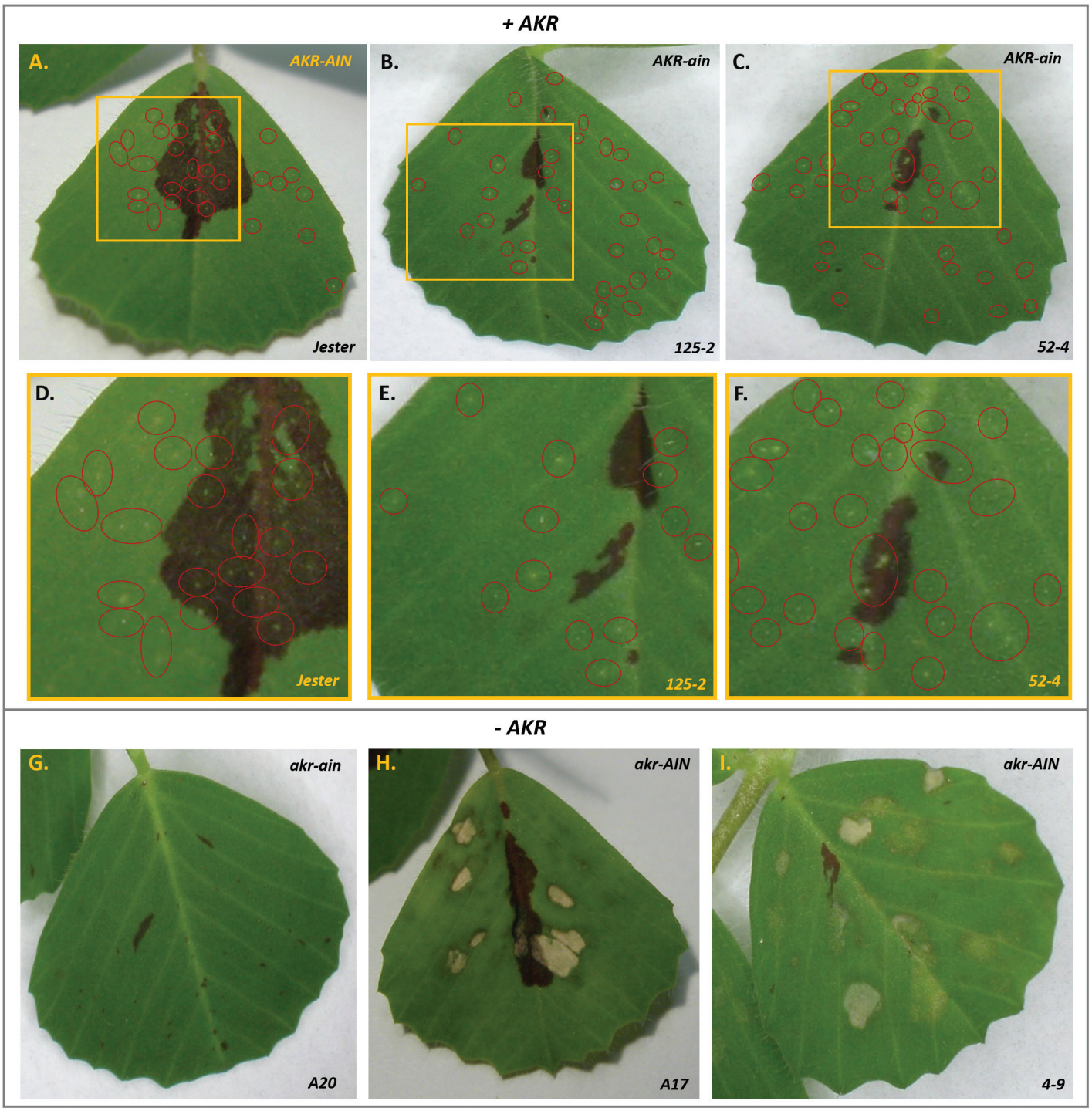

Fig. 3. Damage phenotypes of *M. truncatula* leaflets after 3 d of BGA infestation, according to the haplotype for *AKR* and *AIN* loci. Inbred line or representative $F_{3:4}$ family and haplotypes are indicated at the lower right corner. Chlorotic flecks are present in all the lines carrying *AKR*, irrespective of the presence of *AIN* (A–C), and are circled in red. Zooming in on the leaves of the *AKR–AIN* and *AKR–ain* haplotypes (D–F) highlights the small flecks where BGA has been probing. In the absence of *AKR*, lines carrying *AIN* establish macroscopic necrotic lesions (H, I). Leaflets are ~1.5 cm in width and aphids were removed before photography.

results, *PR1* showed significantly higher transcript abundance following BGA infestation in A20, compared with the non-infested controls of A20, A17, and Jester plants; this increase was similar to that observed in A17, which was significantly lower than the increase observed in Jester following BGA infestation (Fig. 7C).

Most of the genes involved in the JA biosynthetic octadecanoid pathway previously tested were shown to be exclusively induced in the resistant accession Jester following BGA infestation (Gao *et al.*, 2007*a*). Two of the lipoxygenase genes (*LOX2* and *LOX3*) were monitored for their response following BGA infestation in A20 and compared with Jester

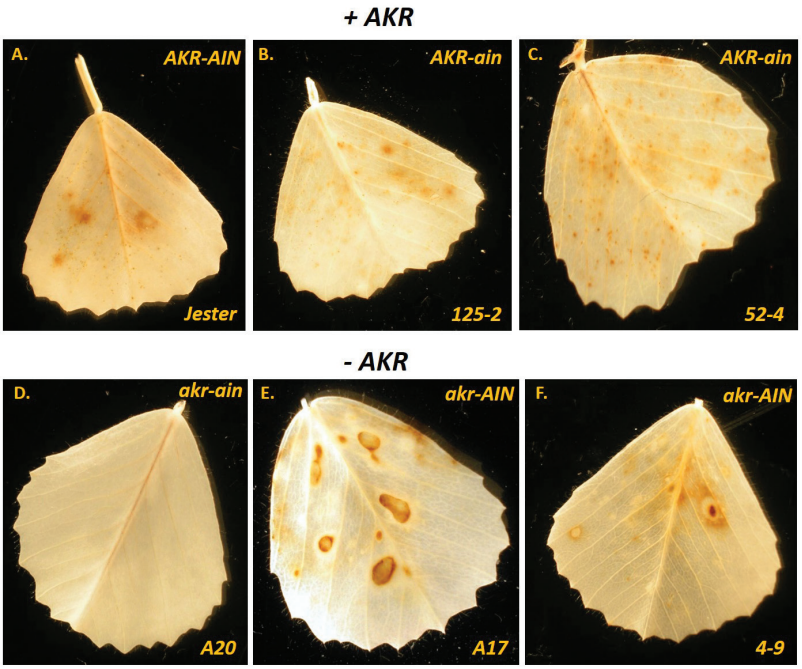

Fig. 4. DAB-stained leaves show H_2O_2 production after 3 d of BGA infestation. Overall, lines carrying the *AKR* locus show small localized spotted DAB staining (A–C) whilst *AIN* alone results in larger necrotic lesions (E, F). No H_2O_2 can be detected when neither *AKR* nor *AIN* is present (D).

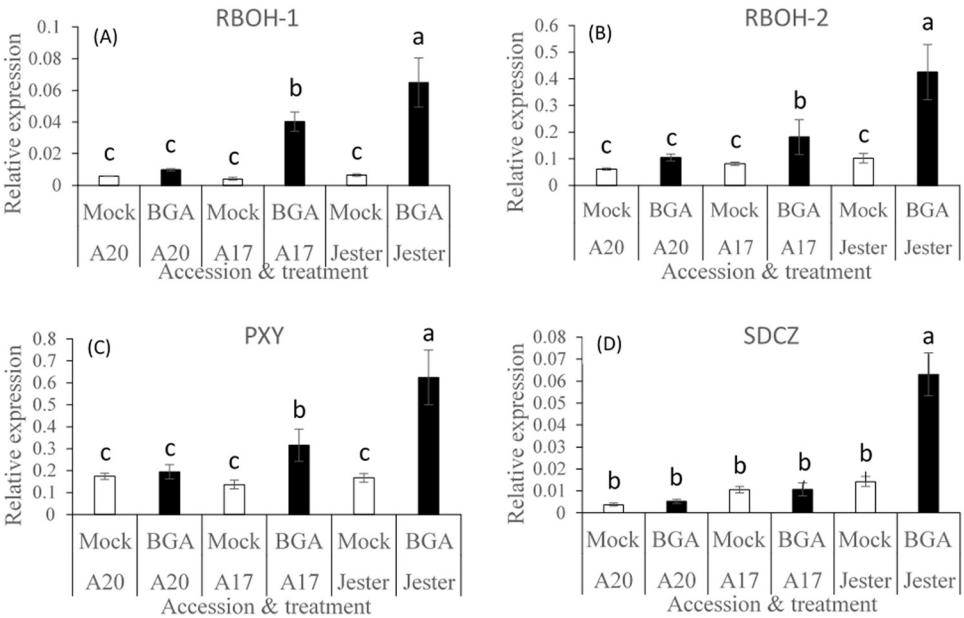

Fig. 5. Transcript accumulation of genes involved in H_2O_2 metabolism (A–D) in uninfested petioles (mock) and BGA-infested petioles of *M. truncatula* accessions A20, A17, and Jester 36 h post-treatment (A) RBOH-1 (respiratory burst oxidase homolog-1); (B) RBOH-2 (respiratory burst oxidase homolog-2); (C) PXY (Peroxidase); and (D) SDCZ (Superoxide dimustase Cu-Zn). The gene identifiers and primer sequences are summarized in Supplementary Table S3. Values are the mean and SE of three biological replicates. Different letters indicate significant differences in transcript abundance determined by Tukey–Kramer HSD test ($P<0.05$).

and A17; no transcriptional change was observed in A17 and A20, whereas significantly higher lipoxygenase transcript abundances were observed in the resistant cv. Jester (Fig. 8A, B). To investigate whether downstream JA-responsive genes were induced, the expression of vegetative storage protein (*VSP*) and proteinase inhibitor (*PI*) was studied. As observed for *LOX2* and *LOX3*, the *VSP* and *PI* genes were only induced in the resistant accession Jester following BGA infestation and not in A17 or A20 (Fig. 8C, D).

The JA signaling pathway is recruited by AKR *following BGA infestation and is not dependent on the presence of* AIN

The contrasting interactions between *AKR* and *AIN* suggest a complex interplay between the molecular events leading to macroscopic necrosis and BGA resistance. To determine the role of the JA and SA defense signaling pathways in the different haplotypes (i.e. *akr–ain*, *akr–AIN*, *AKR–ain*, and

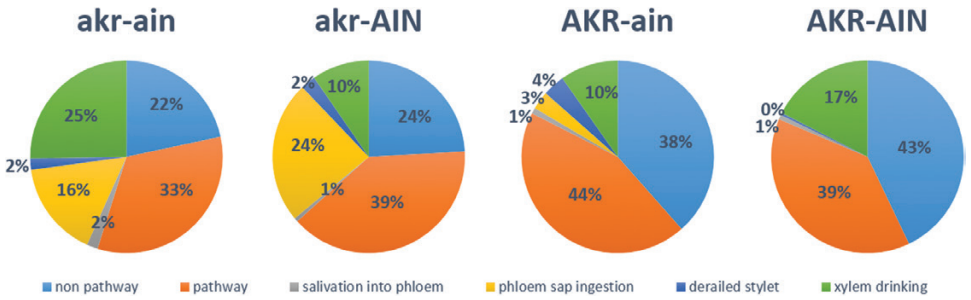

Fig. 6. EPG analysis shows that the *AKR* locus is essential to inhibit phloem sap feeding, irrespective of *AIN*. Feeding behavior was followed for 8 h and the resulting waveform patterns were assigned to six categories with the mean proportion of time spent in each behavior shown for the four haplotypes (a minimum of 12 biological repeats with at least three different lines resulting from the Jester×A20 crosses). Aphids spent significantly ($P<0.05$) more time in the non-pathway category in *AKR* lines and successfully reduce or inhibit phloem feeding when compared with the *akr–ain* and *akr–AIN* haplotypes ($P<0.05$).

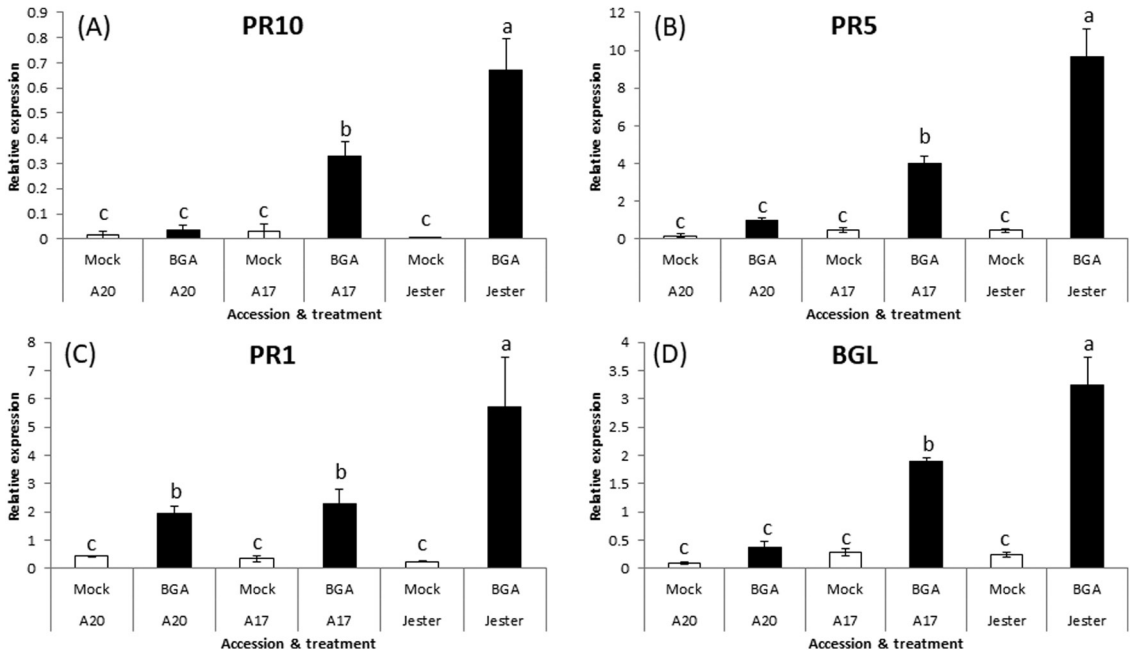

Fig. 7. Transcript accumulation of genes downstream of the salicylic acid signaling pathway (A–D) in uninfested petioles (mock) and BGA-infested petioles of *M. truncatula* accessions A20, A17, and Jester. The gene identifier and primer sequences were the same as described in Gao *et al.* (2007*a*). Values are the mean and SE of three biological replicates. Different letters indicate significant differences in transcript abundance determined by Tukey–Kramer HSD test ($P<0.05$).

AKR–AIN), transcript levels of four SA-responsive and four JA-responsive genes were measured at 36 h following BGA infestation.

The octadecanoid pathway genes, *LOX2* and *LOX3*, and the JA-inducible genes, *VSP* and *PI*, all showed increased transcript abundance in the haplotypes harboring the *AKR* locus (e.g. *AKR–AIN* and *AKR–ain*; Fig. 9A, B) compared with their uninfested controls or plants with the haplotypes *akr–AIN* or *akr–ain* (Fig. 9C, D). The expression of all JA-related genes did not significantly differ between the uninfested plants for all haplotypes. It thus appears that *AKR* alone is sufficient to recruit the JA signaling pathway in the resistance response to BGA.

Since crosstalk is often observed between the JA and SA pathways, we studied the transcript abundances of the SA-inducible genes *PR10*, *PR5*, *PR1*, and *BGL* in the four haplotypes to see whether the recruitment of the JA pathway by *AKR* affects expression of these SA-inducible genes. Overall, and in contrast to the JA-related genes, the four SA-related genes were induced by BGA infestation in all four haplotypes but, similar to the JA-related genes, the response was generally increased by the presence of *AKR* (Fig. 10). With the exception of *PR1*, the results indicate that *AIN* had no effect on these SA-related genes in response to BGA. In the case of *PR1*, the presence of *AIN* in the *AKR* background appeared to attenuate induction by BGA (Fig. 10C).

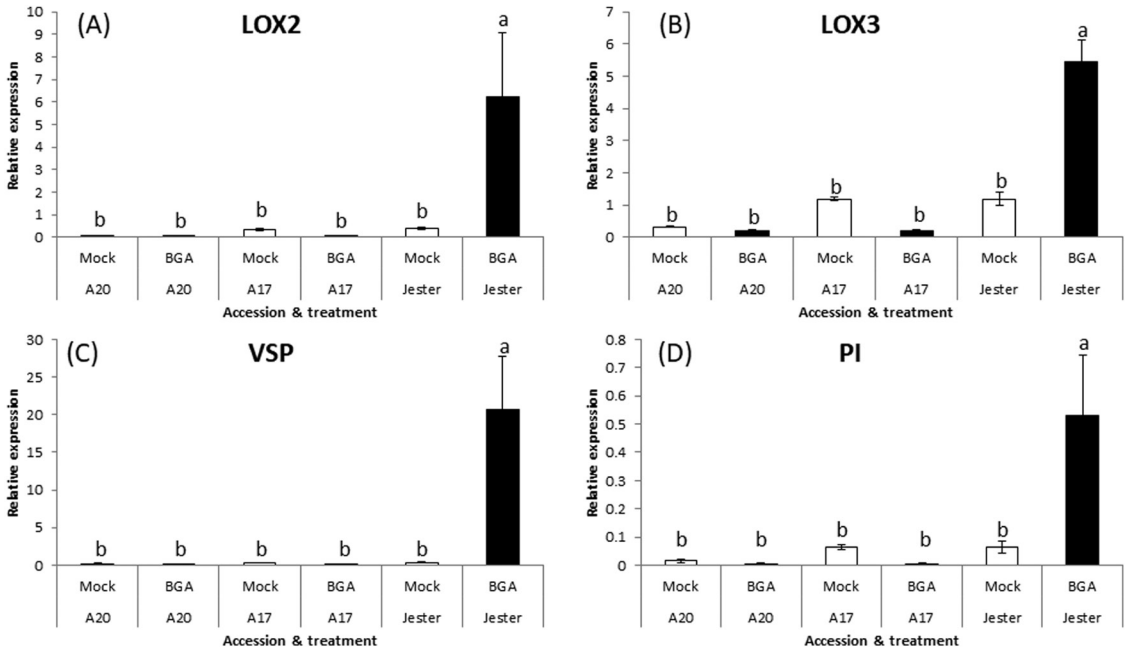

Fig. 8. Transcript accumulation of genes of the octadecanoid pathway (A, B) and genes downstream of the jasmonic acid signaling pathway (C, D) in uninfested petioles (mock) and BGA-infested petioles of *M. truncatula* accessions A20, A17, and Jester. The gene identifier and primer sequences were the same as described in Gao *et al.* (2007*a*). Values are the mean and SE of three biological replicates. Different letters indicate significant differences in transcript abundance by Tukey–Kramer HSD test ($P<0.05$).

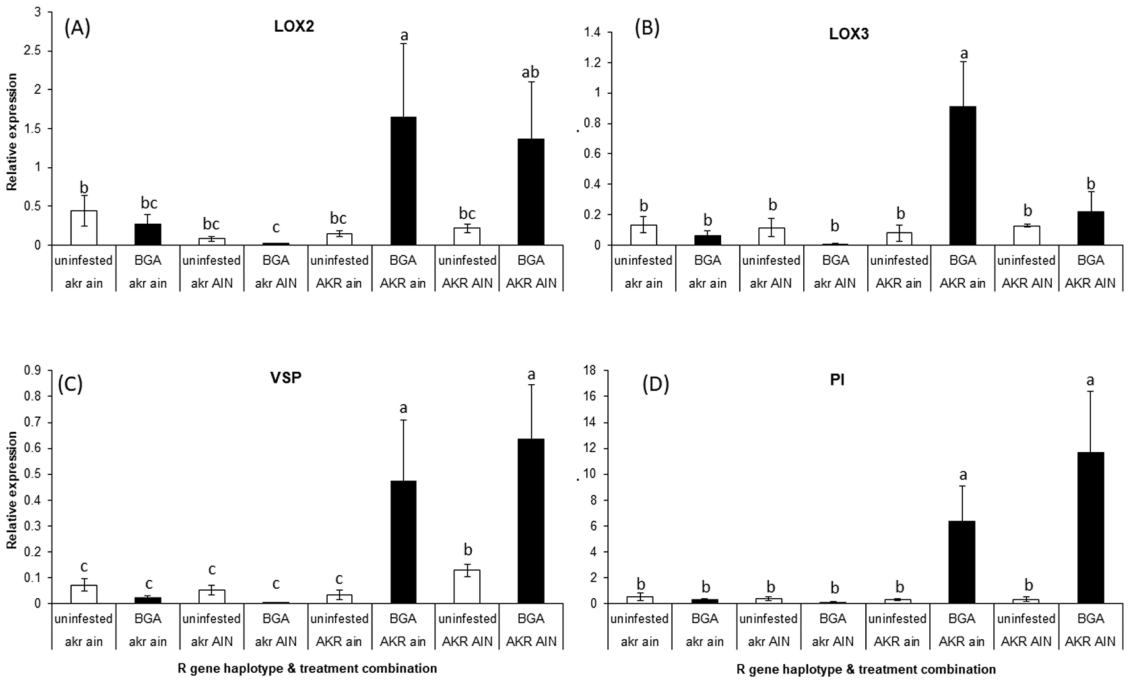

Fig. 9. Transcript accumulation of genes of the octadecanoid pathway (A, B) and genes downstream of the jasmonic acid signaling pathway (C, D) in uninfested (mock) and BGA-infested petioles of *M. truncatula* Jester×A20 $F_{3:4}$ lines with the different haplotype combinations of the *AKR* and *AIN* genes. The gene identifier and primer sequences were the same as described in Gao *et al.* (2007*a*). Values are the mean and SE of three biological replicates from petioles pooled from three different $F_{3:4}$ families for each haplotype. Different letters indicate significant differences in transcript abundance by Tukey–Kramer HSD test ($P<0.05$).

Discussion

Two distinct interactions were observed between the *AIN* and *AKR* genes. With respect to BGA resistance, the two genes appear to be additive in their effects on the aphid population 19 d post-infestation (Fig. 2). In contrast, with respect to the macroscopic necrosis and plant stunting induced by BGA, the *AKR* gene exerts dominant suppression epistasis on *AIN* and allows only for the development of small chlorotic lesions that are, nonetheless, indicative of hypersensitivity to BGA (Figs 3, 4). Heavy infestation of genotype A17 with BGA can lead to

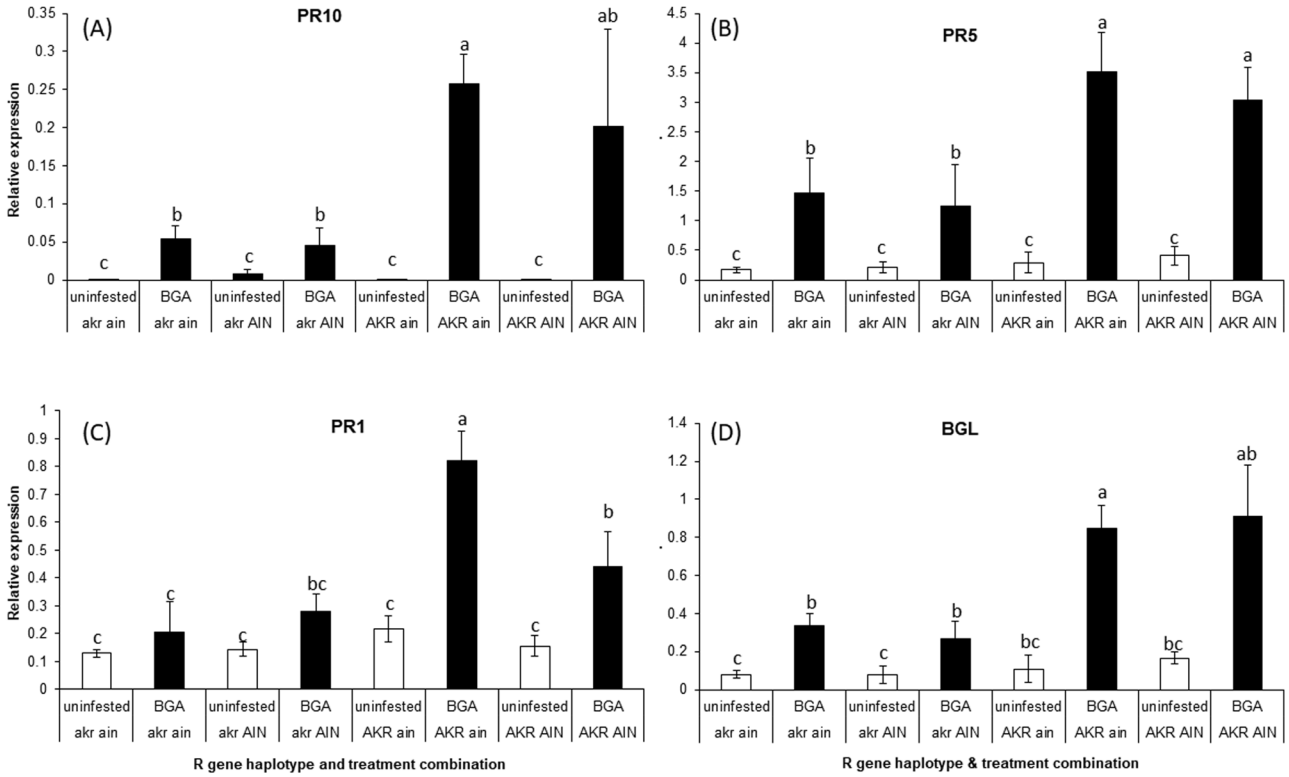

Fig. 10. Transcript accumulation of genes downstream of the salicylic acid signaling pathway (A–D) in uninfested petioles (mock) and BGA-infested petioles of *M. truncatula* Jester×A20 F_4 lines with the different haplotypes combinations of the *AKR* and *AIN* genes. The gene identifier and primer sequences were the same as described in Gao *et al.* (2007*a*). Values are the mean and SE of three biological replicates from petioles pooled from three different F_4 families for each haplotype. Different letters indicate significant differences in transcript abundance by Tukey–Kramer HSD test ($P<0.05$). Error bars are ±SE.

severe plant stunting and death of entire leaves (Klingler *et al.*, 2005, 2009), yet the results of this study show that *AKR* almost completely blocks the development of this syndrome.

The contrasting interactions between *AKR* and *AIN* suggest a complex interplay between the molecular events leading to macroscopic necrosis and BGA resistance. *AIN* appears to enhance the growth of necrotic lesions in the *AKR* background phenotype, as shown in Fig. 2B, although one could speculate that this could also be an indirect effect of less BGA feeding, which warrants further research. Since the combination of these two genes enhances BGA resistance, it is possible that they act in tandem to modulate and optimize the HR.

To our knowledge, this is the first demonstrated example of epistasis between resistance genes against phloem feeding insects. However, at least one instance of a different type of epistatic interaction between insect resistance loci has been reported. Resistance to the bean pod weevil (*Apion godmani* Wagner) is conditioned by two dominant genes in common bean (*Phaseolus vulgaris* L.), one of which gives partial resistance when present alone, and a higher level of resistance in the presence of the additional gene that, by itself, has no effect on resistance (Garza *et al.*, 1996). Furthermore, resistance to Russian wheat aphid in an American barley germplasm line also appears to be controlled by two dominant loci, where one locus confers a high level of resistance and the other allele an intermediate level of resistance only when recessive alleles are present at the first locus, suggesting a possible interaction between the two loci (Mornhinweg *et al.*, 2002). Interestingly, this type of resistance also involves a hypersensitive response, wherein necrosis develops around the site of weevil oviposition and prevents the emerging larva from entering the seed pod (Garza *et al.*, 2001).

Aphids' mode of herbivory bears resemblance, in many respects, to microbial infection of plants. It is notable that both BGA resistance genes reside within clusters of *R* gene-like sequences of the CC-NBS-LRR subfamily (Klingler *et al.*, 2005, 2009). In other plant species, these types of *R* genes encode sensor proteins that mediate resistance phenotypes involving HR against pathogens (Jones and Dangl, 2006). Resistance to cotton-melon aphid (*A. gossypii*) in melon (*Cucumis melo*) is conditioned by a dominant CC-NBS-LLR gene called *Vat* (Dogimont *et al.*, 2014), which was shown to elicit microscopic HR in response to cotton-melon aphid feeding (Villada *et al.*, 2009), reminiscent of the damage observed in the *AKR*-mediated response to BGA in the present study. The necrotic fleck phenotype mediated by *AIN* in response to *Acyrthosiphon* species may arise from pathways homologous to those underlying disease lesion mimic mutants (Bruggeman *et al.*, 2015). A well-studied example is the *Arabidopsis thaliana lsd1* (lesions simulating disease 1) mutant, which knocks out a protein that suppresses cell death in response to pathogens (Aviv *et al.*, 2002) Details from such systems may offer clues to pathways involved in *AIN*-mediated necrotic flecks and the epistatic interaction with *AKR*.

In *M. truncatula* A20, which lacks both the BGA resistance genes *AKR* and *AIN*, the SA-regulated genes *PR10*, *PR5*, and

BGL were not induced following BGA infestation, whereas the *PR1* gene was induced (Fig. 7). Interestingly, when *M. truncatula* is infested with pea aphid, SA is produced in both compatible and incompatible interactions, whereas JA is also produced, although highly variably between treatments and time points (Stewart *et al.*, 2016). The increased production in SA was observed at the site of pea aphid infestation in all interactions and not systemically, where a stronger SA increase was observed in incompatible interactions compared with compatible interactions (Stewart *et al.*, 2016). In another legume, soybean (*Glyine max*), SA-responsive genes are induced in compatible and incompatible interactions, where temporal expression differences of *PR1* were observed in resistant and susceptible soybean lines (Li *et al.*, 2008; Studham and MacIntish, 2013). In Arabidopsis, the expression of SA biosynthetic or signaling genes (*SID2*, *EDS5*, and *PAD4*) is induced in response to green peach aphid (GPA; *Myzus persicae*) feeding (Pegadaraju *et al.*, 2005). However, loss-of-function mutations in the *SID2*, *EDS5*, and *NPR1* genes, which are required for SA signaling, do not compromise resistance to GPA (Moran and Thompson, 2001). In contrast, the *pad4* mutant showed enhanced susceptibility to GPA (Pegadaraju *et al.*, 2005; Louis *et al.*, 2012). PAD4 protein functions together with its interacting partner EDS1 to promote SA-dependent defense response; Louis *et al.* (2012) showed that the PAD4-mediated defense response is SA independent. In both Arabidopsis and tomato, *PR1* expression was observed in compatible interactions following aphid infestation (Martinez de Ilarduya *et al.*, 2003; De Vos *et al.*, 2005). The response observed in A20 thus appears to show similarities to the basal defense against aphids in Arabidopsis, soybean, and tomato. It remains unclear whether SA signaling plays an important role in basal resistance to BGA in *M. truncatula* and perhaps the observations in A20 are an equilibrium between basal defense and effector-triggered susceptibility responses beneficial to BGA. The SA signaling pathway is known to play a major role in the plant HR against pathogens (Torres *et al.*, 2005; Klessig *et al.*, 2018). Here we compared BGA-induced gene expression between A20, A17, and Jester, and concluded that certain aspects of SA signaling are activated in all three accessions (Fig. 7), whereas JA signaling is exclusively activated in Jester (Fig. 7), showing that *AKR*-mediated resistance to BGA in Jester involves JA signaling. Jester harbors both *AKR* and *AIN*, but here we show that the recruitment of JA signaling during BGA infestation is not dependent on the presence of *AIN* (Fig. 8). The absence of *AIN* in an *AKR* background also did not appear to significantly attenuate the transcript abundance of the SA-regulated genes (Figs 9, 10). Despite these observations, it is possible that the pronounced attenuation of macroscopic necrosis in Jester may reflect an *AKR*-mediated antagonism between JA and different branches of SA signaling or generation of reactive oxygen species (ROS) upon BGA infestation, although we demonstrated that H_2O_2-associated genes were up-regulated in both Jester and A17 plants following BGA infestation (Fig. 5).

The EPG analysis showed a significant reduction in phloem feeding on lines harboring *AKR*, irrespective of the presence of *AIN*. This observation could be linked to the JA pathway recruitment by the product of *AKR*. Since feeding behavior was only measured for the initial 8 h of contact, the JA signaling pathway might be a quick and effective means for *AKR* lines to deter aphids from feeding. The early-stage inhibition of phloem feeding may then be complemented over a period of days by the action of *AIN*.

The necrotic flecks and the stunting of *akr–AIN* plants may reflect a resistance mechanism involving ROS that, ultimately, can be harmful to the host plant when overproduced, leading to the reduced biomass of BGA-infested plants that harbor *AIN* (Fig. 2). However, Guo *et al.* (2012) identified a QTL on chromosome 3, separate from both *AIN* and *AKR*, that accounted for 33% in the relative reduction of plant biomass in response to BGA in an A17×A20 recombinant inbred line population. Whether this locus interacts with *AIN*-generated ROS in the same fashion to lead to the reduction in plant biomass remains to be determined. What is clear is that the addition of *AKR* to the *AIN* background may create a much stronger resistance; this enhancement may operate, in part, through a more optimal modulation of ROS homeostasis in aphid-infested leaves. ROS are increasingly recognized for their central role in linking environmental stimuli with plant metabolism, including roles in long-distance signaling (Waszczak *et al.*, 2018). In this regard, it is notable that *AKR*-mediated resistance to BGA was shown to be systemically induced by prior infestation (Klingler *et al.*, 2005), although other systemic signals (including JA-related compounds) may be involved. The production of H_2O_2 in response to BGA, and the genetic interactions underlying the growth of necrotic lesions in the *AIN* background, coupled with the many genetic and genomic resources in the model legume *M. trucatula*, suggest that this system could offer agriculturally relevant clues to ROS biology.

The *M. truncatula* accessions Mogul and Caliph also possess *AKR*, and both appear to lack *AIN* since no macroscopic necrotic lesions or small chlorotic lesions are observed in these accessions, whereas their near-isogenic partners Borung and Cyprus, respectively, lack *AKR* (Gao *et al.*, 2007*b*; Klingler *et al.*, 2007). The use of these additional two pairs of near-isogenic lines with different genetic backgrounds could shed more light on the molecular events that mediate aphid resistance by *AKR* and the influence the presence of *AIN* has on *AKR* activity. The *M. truncatula*–BGA interaction offers the advantage of a genome sequence available for both the plant (Young *et al.*, 2011) and the pea aphid (IAGC, 2010), a congener of BGA, and future endeavors should offer new insights to how plant *R* genes and the HR mediate resistance against insects.

Supplementary data

Supplementary data are available at *JXB* online.

Fig. S1. Relative quantification of DAB-stained leaves from representative $F_{3:4}$ families following 3 d of infestation with BGA.

Table S1. List of the Jester×A20-derived F_3 families and their different *AKR* and *AIN* haplotypes.

Table S2. Overview of the two-sample *t*-test *P*-values for each mean value EPG signal derived from individuals of the four haplotypes of *AKR* and *AIN* (a minimum of 12 biological repeats with at least three different lines resulting from the Jester×A20 crosses).

Table S3. Overview of gene identifiers and qPCR primer sequences of genes in the *M. truncatula* genome involved in H_2O_2 metabolism.

Acknowledgements

We would like to thank Elaine Smith and Jenny Reidy-Croft for technical assistance on the project. SJ is the recipient of a CSIRO OCE-Postdoctoral Fellowship.

References

Aviv DH, Rustérucci C, Holt BF 3rd, Dietrich RA, Parker JE, Dangl JL. 2002. Runaway cell death, but not basal disease resistance, in lsd1 is SA- and NIM1/NPR1-dependent. The Plant Journal **29**, 381–391.

Boissot N, Schoeny A, Vanlerberghe-Masutti F. 2016. *Vat*, an amazing gene conferring resistance to aphids and viruses they carry: from molecular structure to field effects. Frontiers in Plant Science **7**, 1420.

Botha AM, van Eck L, Burger NF, Swanevelder ZH. 2014. Near-isogenic lines of *Triticum aestivum* with distinct modes of resistance exhibit dissimilar transcriptional regulation during *Diuraphis noxia* feeding. Biology Open **3**, 1116–1126.

Bruggeman Q, Raynaud C, Benhamed M, Delarue M. 2015. To die or not to die? Lessons from lesion mimic mutants. Frontiers in Plant Science **6**, 24.

De Vos M, Van Oosten VR, Van Poecke RM, *et al*. 2005. Signal signature and transcriptome changes of *Arabidopsis* during pathogen and insect attack. Molecular Plant-Microbe Interactions **18**, 923–937.

Dogimont C, Chovelon V, Pauquet J, Boualem A, Bendahmane A. 2014. The *Vat* locus encodes for a CC-NBS-LRR protein that confers resistance to *Aphis gossypii* infestation and *A. gossypii*-mediated virus resistance. The Plant Journal **80**, 993–1004.

Escudero-Martinez CM, Morris JA, Hedley PE, Bos JIB. 2017. Barley transcriptome analyses upon interaction with different aphid species identify thionins contributing to resistance. Plant, Cell & Environment **40**, 2628–2643.

Gao LL, Anderson JP, Klingler JP, Nair RM, Edwards OR, Singh KB. 2007*a*. Involvement of the octadecanoid pathway in bluegreen aphid resistance in *Medicago truncatula*. Molecular Plant-Microbe Interactions **20**, 82–93.

Gao LL, Horbury R, Nair RM, Singh KB, Edwards OR. 2007*b*. Characterization of resistance to multiple aphid species (Hemiptera: Aphididae) in *Medicago truncatula*. Bulletin of Entomological Research **97**, 41–48.

Gao LL, Kamphuis LG, Kakar K, Edwards OR, Udvardi MK, Singh KB. 2010. Identification of potential early regulators of aphid resistance in *Medicago truncatula* via transcription factor expression profiling. New Phytologist **186**, 980–994.

Gao LL, Klingler JP, Anderson JP, Edwards OR, Singh KB. 2008. Characterization of pea aphid resistance in *Medicago truncatula*. Plant Physiology **146**, 996–1009.

Garza R, Cardona C, Singh SP. 1996. Inheritance of resistance to the bean-pod weevil (*Apion godmani* Wagner) in common beans from Mexico. Theoretical and Applied Genetics **92**, 357–362.

Garza R, Vera J, Cardona C, Barcenas N, Singh SP. 2001. Hypersensitive response of beans to *Apion godmani* (Coleoptera: Curculionidae). Journal of Economic Entomology **94**, 958–962.

Goggin FL. 2007. Plant–aphid interactions: molecular and ecological perspectives. Current Opinion in Plant Biology **10**, 399–408.

Guo S, Kamphuis LG, Gao L, Edwards OR, Singh KB. 2009. Two independent resistance genes in the *Medicago truncatula* cultivar jester confer resistance to two different aphid species of the genus *Acyrthosiphon*. Plant Signaling & Behavior **4**, 328–331.

Guo SM, Kamphuis LG, Gao LL, Klingler JP, Lichtenzveig J, Edwards O, Singh KB. 2012. Identification of distinct quantitative trait loci associated with defence against the closely related aphids *Acyrthosiphon pisum* and *A. kondoi* in *Medicago truncatula*. Journal of Experimental Botany **63**, 3913–3922.

Hill CB, Shiao D, Fox CM, Hartman GL. 2017. Characterization and genetics of multiple soybean aphid biotype resistance in five soybean plant introductions. Theoretical and Applied Genetics **130**, 1335–1348.

Hill J. 2000. Jester. Plant Varieties Journal **13**, 40.

IAGC. 2010. Genome sequence of the pea aphid *Acyrthosiphon pisum*. PLoS Biology **8**, e1000313.

Jaouannet M, Morris JA, Hedley PE, Bos JI. 2015. Characterization of *Arabidopsis* transcriptional responses to different aphid species reveals genes that contribute to host susceptibility and non-host resistance. PLoS Pathogens **11**, e1004918.

Jones JD, Dangl JL. 2006. The plant immune system. Nature **444**, 323–329.

Kamphuis LG, Gao L, Singh KB. 2012. Identification and characterization of resistance to cowpea aphid (*Aphis craccivora* Koch) in *Medicago truncatula*. BMC Plant Biology **12**, 101.

Kamphuis LG, Guo SM, Gao LL, Singh KB. 2015. Genetic mapping of a major resistance gene to pea aphid (*Acyrthosipon pisum*) in the model legume *Medicago truncatula*. International Journal of Molecular Sciences **17**, E1224.

Kamphuis LG, Lichtenzveig J, Peng K, *et al*. 2013*a*. Physiology and genetics of resistance to spotted alfalfa aphid (*Therioaphis trifolii*) in *Medicago truncatula*. Journal of Experimental Botany **64**, 5157–5172.

Kamphuis LG, Williams AH, D'Souza NK, Pfaff T, Ellwood SR, Groves EJ, Singh KB, Oliver RP, Lichtenzveig J. 2007. The *Medicago truncatula* reference accession A17 has an aberrant chromosomal configuration. New Phytologist **174**, 299–303.

Kamphuis LG, Zulak K, Gao L-L, Anderson JP, Singh KB. 2013*b*. Plant–aphid interactions with a focus on legumes. Functional Plant Biology **40**, 1271–1284.

Klessig DF, Choi HW, Dempsey DA. 2018. Systemic acquired resistance and salicylic acid: past, present, and future. Molecular Plant-Microbe Interactions **31**, 871–888.

Klingler J, Creasy R, Gao L, Nair RM, Calix AS, Jacob HS, Edwards OR, Singh KB. 2005. Aphid resistance in *Medicago truncatula* involves antixenosis and phloem-specific, inducible antibiosis, and maps to a single locus flanked by NBS-LRR resistance gene analogs. Plant Physiology **137**, 1445–1455.

Klingler JP, Edwards OR, Singh KB. 2007. Independent action and contrasting phenotypes of resistance genes against spotted alfalfa aphid and bluegreen aphid in *Medicago truncatula*. New Phytologist **173**, 630–640.

Klingler JP, Nair RM, Edwards OR, Singh KB. 2009. A single gene, *AIN*, in *Medicago truncatula* mediates a hypersensitive response to both bluegreen aphid and pea aphid, but confers resistance only to bluegreen aphid. Journal of Experimental Botany **60**, 4115–4127.

Li Y, Zou J, Li M, Bilgin DD, Vodkin LO, Hartman GL, Clough SJ. 2008. Soybean defense responses to the soybean aphid. New Phytologist **179**, 185–195.

Louis J, Gobbato E, Mondal HA, Feys BJ, Parker JE, Shah J. 2012. Discrimination of Arabidopsis PAD4 activities in defense against green peach aphid and pathogens. Plant Physiology **158**, 1860–1872.

Martinez de Ilarduya O, Xie Q, Kaloshian I. 2003. Aphid-induced defense responses in *Mi-1*-mediated compatible and incompatible tomato interactions. Molecular Plant-Microbe Interactions **16**, 699–708.

Moran PJ, Thompson GA. 2001. Molecular responses to aphid feeding in Arabidopsis in relation to plant defense pathways. Plant Physiology **125**, 1074–1085.

Mornhinweg DW, Porter DR, Webster JA. 2002. Inheritance of Russian wheat aphid resistance in spring barley germplasm line STARS-9577B. Crop Science **42**, 1891–1893.

O'Neal ME, Varenhorst AJ, Kaiser MC. 2018. Rapid evolution to host plant resistance by an invasive herbivore: soybean aphid (*Aphis glycines*) virulence in North America to aphid resistant cultivars. Current Opinion in Insect Science **26**, 1–7.

Orozco-Cardenas M, Ryan CA. 1999. Hydrogen peroxide is generated systemically in plant leaves by wounding and systemin via the octadecanoid pathway. Proceedings of the National Academy of Sciences, USA **96**, 6553–6557.

Pegadaraju V, Knepper C, Reese J, Shah J. 2005. Premature leaf senescence modulated by the Arabidopsis PHYTOALEXIN DEFICIENT4 gene is associated with defense against the phloem-feeding green peach aphid. Plant Physiology **139**, 1927–1934.

Rossi M, Goggin F, Milligan SB, *et al*. 1998. The nematode resistance gene *Mi* of tomato confers resistance against the potato aphid. Proceedings of the National Academy of Sciences, USA **95**, 9750–9754.

Song J, Liu H, Zhuang H, Zhao C, Xu Y, Wu S, Qi J, Li J, Hettenhausen C, Wu J. 2017. Transcriptomics and alternative splicing analyses reveal large differences between maize lines B73 and Mo17 in response to aphid *Rhopalosiphum padi* infestation. Frontiers in Plant Science **8**, 1738.

Sosa JM, Huber DE, Welk B, Fraser HL. 2014. Development and application of MIPAR™: a novel software package for two- and three-dimensional microstructural characterization. Integrating Materials **3**, 10.

Stewart SA, Hodge S, Bennett M, Mansfield JW, Powell G. 2016. Aphid induction of phytohormones in *Medicago truncatula* is dependent upon time post-infestation, aphid density and the genotypes of both plant and insect. Anthropod-Plant Interactions **10**, 51–53.

Stewart SA, Hodge S, Ismail N, Mansfield JW, Feys BJ, Prospéri JM, Huguet T, Ben C, Gentzbittel L, Powell G. 2009. The *RAP1* gene confers effective, race-specific resistance to the pea aphid in *Medicago truncatula* independent of the hypersensitive reaction. Molecular Plant-Microbe Interactions **22**, 1645–1655.

Studham ME, MacIntosh GC. 2013. Multiple phytohormone signals control the transcriptional response to soybean aphid infestation in susceptible and resistant soybean plants. Molecular Plant-Microbe Interactions **26**, 116–129.

Thompson GA, Goggin FL. 2006. Transcriptomics and functional genomics of plant defence induction by phloem-feeding insects. Journal of Experimental Botany **57**, 755–766.

Thordal-Christensen H, Zhang ZG, Wei YD, Collinge DB. 1997. Subcellular localization of H_2O_2 in plants. H_2O_2 accumulation in papillae and hypersensitive response during the barley–powdery mildew interaction. The Plant Journal **11**, 1187–1194.

Tjallingii WF. 1978. Electronic recording of penetration behaviour by aphids. Entomologia Experimentalis et Applicata **24**, 721–730.

Tjallingii WF, Esch TH. 1993. Fine-structure of aphid stylet routes in plant tissues in correlation with EPG signals. Physiological Entomology **18**, 317–328.

Torres MA, Jones JD, Dangl JL. 2005. Pathogen-induced, NADPH oxidase-derived reactive oxygen intermediates suppress spread of cell death in *Arabidopsis thaliana*. Nature Genetics **37**, 1130–1134.

Villada ES, González EG, López-Sesé AI, Castiel AF, Gómez-Guillamón ML. 2009. Hypersensitive response to *Aphis gossypii* Glover in melon genotypes carrying the *Vat* gene. Journal of Experimental Botany **60**, 3269–3277.

Walling LL. 2008. Avoiding effective defenses: strategies employed by phloem-feeding insects. Plant Physiology **146**, 859–866.

Waszczak C, Carmody M, Kangasjärvi J. 2018. Reactive oxygen species in plant signaling. Annual Review of Plant Biology **69**, 209–236.

Wroblewski T, Piskurewicz U, Tomczak A, Ochoa O, Michelmore RW. 2007. Silencing of the major family of NBS-LRR-encoding genes in lettuce results in the loss of multiple resistance specificities. The Plant Journal **51**, 803–818.

Young ND, Debellé F, Oldroyd GE, *et al*. 2011. The *Medicago* genome provides insight into the evolution of rhizobial symbioses. Nature **480**, 520–524.

Züst T, Agrawal AA. 2016. Mechanisms and evolution of plant resistance to aphids. Nature Plants **2**, 15206.